

A Dynamic Quasi-Newton Method for Uncalibrated Visual Servoing

Jenelle Armstrong Piepmeier
Mechanical Engineering
Georgia Institute of Technology
Atlanta, GA 30332-0405

Gary V. McMurray
Georgia Tech Research Institute
Atlanta, GA 30332-0823

Harvey Lipkin
Mechanical Engineering
Georgia Institute of Technology
Atlanta, GA 30332-0405

Abstract

Tracking of a moving target by uncalibrated model independent visual servo control is achieved by developing a new “dynamic” quasi-Newton approach. Model independent visual servo control is defined as using visual feedback to control a robot without precisely calibrated kinematic and camera models. The control problem is formulated as a nonlinear least squares optimization. For the moving target case, this results in a time-varying objective function which is minimized using a new dynamic Newton’s method. A second-order convergence rate is established, and it is shown that the standard method is not guaranteed convergence for a moving target. The algorithm is extended to develop a dynamic Broyden update and subsequently a dynamic quasi-Newton method. Results for both one- and six-degree-of-freedom systems demonstrate the success of the algorithm and shows dramatic improvement over previous methods.

1 Introduction

The model independent approach describes visual servoing algorithms that are independent of hardware (robot and camera systems) types and configuration. The most thorough treatment of such a method has been performed by Jagersand [10], [11]. He formulates the visual servoing problem as a nonlinear least squares problem solved by a quasi-Newton method using Broyden Jacobian estimation. Jagersand demonstrates the robust properties of this type of control. He also demonstrates significantly improved repeatability over standard joint control even on an older robot with backlash. However, this work focuses on servoing a robot end-effector to a static target.

The tracking of moving targets has been addressed by several authors including [1], [2]. However, these control methods are model based; the kinematic model of the robot and the camera system geometry are known.

In [12], the authors demonstrated the limited capability of a quasi-Newton method for tracking moving targets. Target state prediction schemes improved tracking accuracy, but did not improve precision. It is shown here that Newton’s method as applied in [10] and [12] is designed to converge on a static target, and is not guaranteed to converge on a moving target. This paper addresses a moving target scenario giving an objective function in both joint and time variables. The result is a dynamic quasi-Newton control law implementing a dynamic Broyden update that is applicable to the moving target problem without target state prediction.

2 Problem Definition

This paper addresses an *image-based* visual servoing method. According to the classification scheme developed by Sanderson and Weiss [13], the method can be further classified as *dynamic look-and-move*. This means that the algorithm provides joint positions as reference inputs for the joint-level controllers. In addition, the approach is *endpoint closed-loop* (ECL) [9] which refers to the fact that the vision system views both the target and the end-effector. Figure 1 shows the controller block diagram used in [12] and in this paper. Joint positions are calculated using a nonlinear least squares optimization method which minimizes the error in the image plane. The method estimates the Jacobian on-line and does not require calibrated models of either the camera configuration or the robot kinematics.

3 Nonlinear Least Squares for a Moving Target

For a moving target at position $y^*(t)$, and an end-effector at position $y(\theta)$, as seen in the image plane, the residual error between the two points can be expressed as $f(\theta, t) = y(\theta) - y^*(t)$. The objective func-

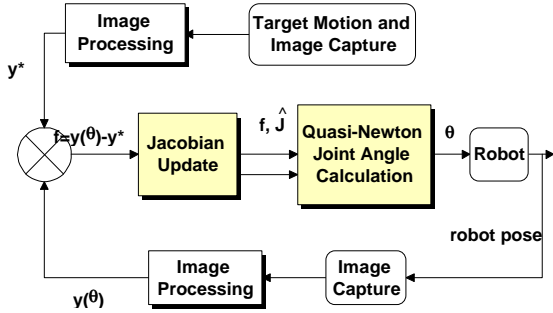


Figure 1: Controller block diagram showing a model-independent approach using a non-linear least squares optimization algorithm. Note that joint angle calculations are made using the optimization algorithm; no inverse kinematics are used.

tion to be minimized, F , is a function of squared error.

$$F(\theta, t) = \frac{1}{2} f^T(\theta, t) f(\theta, t)$$

The Taylor series expansion about θ, t is

$$F(\theta + h_\theta, t + h_t) = F(\theta, t) + F_\theta h_\theta + F_t h_t + \dots$$

where F_θ, F_t are partial derivatives and h_θ, h_t are increments of θ, t . For a fixed sampling period h_t , F is minimized by solving

$$\begin{aligned} 0 &= \frac{\partial F(\theta + h_\theta, t + h_t)}{\partial \theta} \\ 0 &= F_\theta + F_{\theta\theta} h_\theta + F_{t\theta} h_t + O(h_\theta^2) \end{aligned}$$

The term $O(h_\theta^2)$ indicates second order terms where h_t is absorbed into h_θ since it is assumed they are on the same order of magnitude. Dropping the higher order terms yields

$$\begin{aligned} 0 &= F_\theta + F_{\theta\theta} h_\theta + F_{t\theta} h_t \\ h_\theta &= -(F_{\theta\theta})^{-1} (F_\theta + F_{t\theta} h_t) \\ \theta_{k+1} &= \theta_k - (F_{\theta\theta})^{-1} (F_\theta + F_{t\theta} h_t) \end{aligned} \quad (1)$$

where the discretization $h_\theta = \theta_{k+1} - \theta_k$ is introduced. Equation (1) is referred to as the “dynamic” Newton’s method. If the target is static, F is a function of θ and $F_{t\theta} = 0$. This results in the “static” Newton’s method, $\theta_{k+1} = \theta_k - (F_{\theta\theta})^{-1} (F_\theta)$, which is the basis for previous work by [8], [11], and [12].

3.1 Convergence

Following the derivations given in [6], it can be shown that the dynamic Newton’s method converges in the neighborhood of a moving target.

Theorem 1 Assume that $F(\theta, t) \in C^2$, θ_k is in a neighborhood of a local minimizer θ^* , and $F_{\theta\theta}(\theta^*)$ is positive definite, then a dynamic Newton’s method is well defined for all θ_k , and converges at second order.

Proof. Define the dynamic Newton’s method as

$$h_\theta = -(F_{\theta\theta})^{-1} (F_\theta + F_{t\theta} h_t) \quad (2)$$

where $h_\theta = \theta_{k+1} - \theta_k$ is the commanded change in joint angles at the k th iteration. Let θ^* be the minimum error solution and $h_\theta^* = \theta^* - \theta_k$ for a given h_t . At θ^* the gradient is zero.

$$0 = F_\theta + F_{\theta\theta} h_\theta^* + F_{t\theta} h_t + O(h_\theta^{*2})$$

Multiplying through by $(F_{\theta\theta})^{-1}$ gives

$$\begin{aligned} 0 &= (F_{\theta\theta})^{-1} F_\theta + h_\theta^* + (F_{\theta\theta})^{-1} F_{t\theta} h_t + O(h_\theta^{*2}) \\ &= (F_{\theta\theta})^{-1} (F_\theta + F_{t\theta} h_t) + h_\theta^* + O(h_\theta^{*2}) \end{aligned} \quad (3)$$

and substituting terms from (2) yields

$$\begin{aligned} 0 &= -h_\theta + h_\theta^* + O(h_\theta^{*2}) \\ h_\theta - h_\theta^* &= O(h_\theta^{*2}) \\ \|h_\theta - h_\theta^*\| &= O(\|h_\theta^*\|^2) \end{aligned}$$

By definition of $O(\cdot)^1$,

$$\|h_\theta - h_\theta^*\| \leq c \|h_\theta^*\|^2 \quad (4)$$

where $c > 0$. If θ_k is in a closer neighborhood for which $\|h_\theta^*\| \leq \alpha/c$ where $0 < \alpha < 1$ then,

$$\|h_\theta - h_\theta^*\| \leq \alpha \|h_\theta^*\|$$

At the k th time,

$$\begin{aligned} \|\theta_{k+1} - \theta_k - (\theta^* - \theta_k)\| &\leq \alpha \|\theta^* - \theta_k\| \\ \|\theta^* - \theta_{k+1}\| &\leq \alpha \|\theta^* - \theta_k\| \end{aligned}$$

Thus θ_{k+1} is in the neighborhood and by induction the iteration is well defined for all k and $\|h_\theta^*\| \rightarrow 0$. The iteration has a second order convergence as shown by (4). ■

¹Let $h \rightarrow 0$: then $a = O(h)$ iff \exists a constant c such that $|a| \leq ch$.

It can also be shown that the static Newton's method may not converge on a moving target by adapting the previous proof. Define the static Newton's method as

$$h_\theta = -(F_{\theta\theta})^{-1}(F_\theta) \quad (5)$$

Substituting this into (3) and following the same procedure gives

$$\begin{aligned} 0 &= -h_\theta + h_\theta^* + F_{\theta\theta}^{-1}F_{t\theta}h_t + O(h_\theta^{*2}) \\ h_\theta - h_\theta^* - F_{\theta\theta}^{-1}F_{t\theta}h_t &= O(h_\theta^{*2}) \\ \|h_\theta - h_\theta^* - F_{\theta\theta}^{-1}F_{t\theta}h_t\| &= O(\|h_\theta^*\|^2) \\ \|h_\theta - h_\theta^* - F_{\theta\theta}^{-1}F_{t\theta}h_t\| &\leq c\|h_\theta^*\|^2 \\ \|h_\theta - h_\theta^*\| - \|F_{\theta\theta}^{-1}F_{t\theta}h_t\| &\leq \alpha\|h_\theta^*\| \end{aligned}$$

resulting in,

$$\|\theta^* - \theta_{k+1}\| \leq \alpha\|\theta^* - \theta_k\| + \|F_{\theta\theta}^{-1}F_{t\theta}h_t\|$$

This implies that the sequence $\theta_k, \theta_{k+1}, \dots$ may not converge to θ^* . However, for a static target, $F = F(\theta)$, and $F_{t\theta} = 0$, and (5) will converge on the static target as expected.

While proof of convergence for the dynamic Newton's method is important, the algorithm presents the same disadvantages as Newton's method: the starting point θ_0 needs to be in the neighborhood of θ^* , the term $F_{\theta\theta}$ is required, and may not be positive definite. The following section addresses modifications motivated by the model-independent paradigm.

3.2 Practical Considerations

A careful look at the terms in the dynamic Newton's method (1) reveals some implementation issues. Expanding f , $F_{\theta\theta}$, and $F_{t\theta}$ results in

$$\theta_{k+1} = \theta_k - (J^T J + S)^{-1} (J^T f - J^T \frac{\partial y^*(t)}{\partial t} h_t)$$

where $S = \frac{\partial J^T}{\partial \theta} f$ and

$$J = \frac{\partial y(\theta)}{\partial \theta}, \text{ the Jacobian}$$

To compute the terms S and J analytically would require a calibrated system model. The term S is difficult to estimate. As θ_k approaches the solution, this term approaches zero. Hence, it is often dropped (also known as the Gauss-Newton method). The convergence properties of a dynamic Gauss-Newton method are similar to the dynamic Newton method provided S is not too large.

The Jacobian J can be replaced by an estimated Jacobian, \hat{J} , using Broyden estimation and the method becomes a quasi-Newton method. The following section proposes a dynamic Broyden's method.

The term $\frac{\partial y^*(t)}{\partial t}$ is the velocity of the target. Since only first order information on the target is available from the vision information, velocity estimates are used.

3.3 Broyden's Method for a Moving Target

Broyden's method is a quasi-Newton method; the algorithm substitutes an estimated Jacobian for the analytic Jacobian based on changes in the error function corresponding to changes in state variables. The estimated Jacobian is a secant approximation to the Jacobian [5]. As with Newton's method, the moving target scenario requires that the appropriate derivatives are included. A dynamic Broyden's method for a moving target scenario can be derived in a similar manner to the dynamic Newton's method given in Section 3 and following the approach taken in [5]. However, for brevity the derivation is omitted here.

Let \hat{J}_k represent the approximation to J_k . For this problem formulation, the Jacobian represents a composite Jacobian including both robot and image Jacobians. The Broyden update, $\Delta \hat{J}$, for a static target scenario is given as follows.

$$\begin{aligned} \Delta \hat{J}_{static} &= \frac{(\Delta f - \hat{J}_k h_\theta) h_\theta^T}{h_\theta^T h_\theta} \\ \Delta f &= f_k - f_{k-1} \end{aligned}$$

The proposed dynamic Broyden update contains an additional term, $\frac{\partial y^*(t)}{\partial t} h_t$.

$$\Delta \hat{J} = \frac{(\Delta f - \hat{J}_k h_\theta + \frac{\partial y^*(t)}{\partial t} h_t) h_\theta^T}{h_\theta^T h_\theta} \quad (6)$$

Notice that if the target stops moving, the term $\frac{\partial y^*(t)}{\partial t} = 0$, and the update term is identical to that for a static target.

Incorporating the dynamic Broyden update with the results of Section 3, and the considerations of Section 3.2, results in the following quasi-Newton approach: a dynamic Broyden's Method given by Algorithm 1.

Algorithm 1 Dynamic Broyden's Method

Given $f : \mathbb{R}^n \rightarrow \mathbb{R}^m; \theta_0, \theta_1 \in \mathbb{R}^n; \hat{J}_0 \in \mathbb{R}^{m \times n}$

Do for $k = 1, 2, \dots$

$$\Delta f = f_k - f_{k-1}$$

$$\hat{J}_k = \hat{J}_{k-1} + \frac{(\Delta f - \hat{J}_{k-1} h_\theta + \frac{\partial y^*(t)}{\partial t} h_t) h_\theta^T}{h_\theta^T h_\theta}$$

$$\theta_{k+1} = \theta_k - \left(\hat{J}_k^T \hat{J}_k \right)^{-1} \hat{J}_k^T \left(f_k - \frac{\partial y^*(t)}{\partial t} h_t \right)$$

While this algorithm is not expected to produce quadratic convergence, the simulation results verify the validity of the approach.

4 Simulation and Results

4.1 1 DOF manipulator

Figure 2 shows a simple one degree-of-freedom (1 DOF) system that has been simulated to test the dynamic controller and Broyden's update method as given by Algorithm 1. An arm fixed to a rotary joint is located $400mm$ from the midpoint of the target motion. An arbitrary sensory system notes the position of the target and where the arm crosses the line of target motion. No noise was added to the sensor data for this simulation. Error is measured as the distance between the arm and the target along the line of target motion.

The target is moving sinusoidally with an amplitude of $250mm$ at $1.5 rad/s$ which results in a maximum speed of $375mm/s$. The simulation is performed with a $50ms$ sampling period. Velocity state estimates are computed by first order differencing of the target position.

Figure 3 shows the tracking errors for both a static and dynamic quasi-Newton controller. The error in Fig. 3A appears chaotic, and contains spikes several orders of magnitude higher than the amplitude of the target motion. The rms error is about $390mm$. The steady-state error in Fig. 3B has an rms value of $1mm$. These results for a one degree-of-freedom system strongly validate the appropriately derived control law and Jacobian update.

4.2 6 DOF manipulator

The one-dimensional sensor-based control example in the previous section demonstrates a significant performance improvement for the tracking of moving targets using dynamic quasi-Newton method and Jacobian estimator. This section describes similar success for visual servo control of a 6-DOF manipulator in simulation. A 6-DOF simulation testbed has been constructed in SIMULINK using the PUMA 560 kinematics provided in the *Robotics Toolbox* by Corke [4].

The camera system consists of a stereo arrangement as described in [12], and $\pm \frac{1}{2}$ pixel quantization noise is added to image data. Controlling six degrees-of-freedom with this system requires tracking

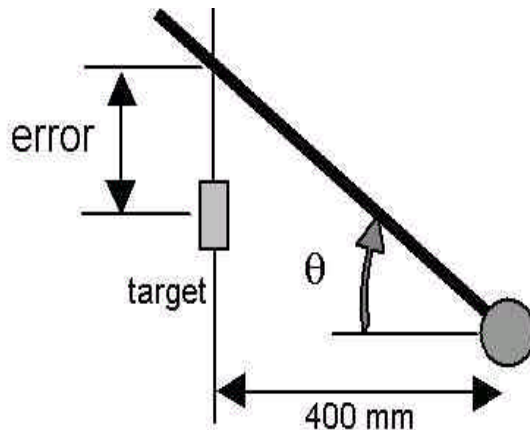


Figure 2: 1-DOF system used to test rederivation of quasi-Newton control law in simulation.

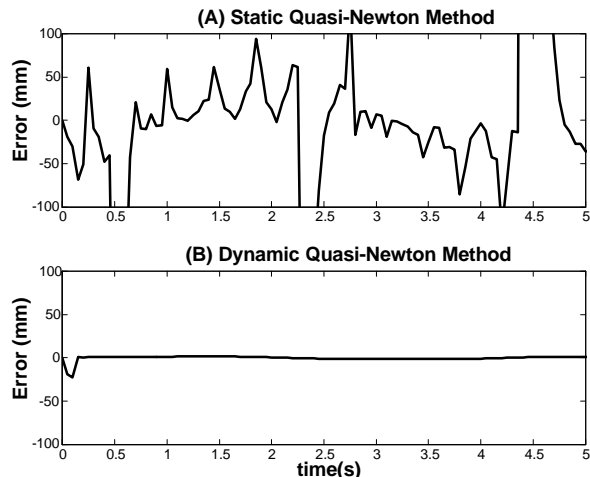


Figure 3: Tracking error for static (A) and dynamic (B) control of an 1-DOF arm tracking a target moving sinusoidally with an amplitude of $250mm$ and a frequency of $1.5rad/s$. The RMS error is in excess of 150% of the target amplitude. The controller derived for a moving target (B) shows significant tracking improvement with RMS error less than 0.4% of the target amplitude.

three points on the end-effector. The simulated target object also consists of three points. The sampling period is $50ms$; the end effector and the target are initially coincident, and the initial Jacobian is perturbed with Gaussian random noise with a variance of 2 pixels/radian . Target velocity estimates are computed using first-order differencing; the simulation has no initial knowledge of the target velocity.

Figure 4 shows the Cartesian error norm between the three end effector points and the three target points. The target object is translating with one point along the coordinate path $[400 \ 0.0 \ 250\sin(1.5t)] \text{ mm}$ with the base of the PUMA 560 located at the origin of the coordinate frame. The end effector converges to a solution after about 5-6 steps. Initial missteps are due to initial conditions: a perturbed initial Jacobian and no initial knowledge about target velocity. The steady-state ($t \geq 1$) rms Cartesian errors are $[3.9 \ 4.5 \ 4.1] \text{ mm}$. This represents a slight increase over the 1-DOF results, however, the 6-DOF problem is more complex and the simulation includes system noise. Figure 5 shows the corresponding three error norms in the image plane, with a steady-state rms error of $[1.1 \ 1.2 \ 1.1] \text{ pixels}$.

Figure 6 shows one target/end effector pair as the target follows a more complex cycloidal path in the Y-Z plane. The maximum speed of the target along this path is 440mm/s . Initial missteps occur as the algorithm is learning; the steady-state rms Cartesian and image errors along this path are $[7.0 \ 6.7 \ 6.9] \text{ mm}$ and $[1.9 \ 1.8 \ 1.7] \text{ pixels}$, respectively. These results demonstrate the ability of this algorithm to control higher order systems and track complex target motions.

5 Summary

The previous two sections clearly demonstrate the tracking ability of the dynamic quasi-Newton algorithm. It is interesting to note that this approach does not require the prediction schemes used in [12], and results in better tracking precision by an order of magnitude. These initial simulation results also show an improvement in image plane target tracking as compared to the model-based approaches taken in [2], [3], and [7].

Repeated simulations show increased sensitivity to initial conditions for the higher-order systems. While they do not affect steady-state behavior, initial conditions can affect the transient behavior (time to convergence). Further work will focus on three issues: improving transient control, quantifying robustness to

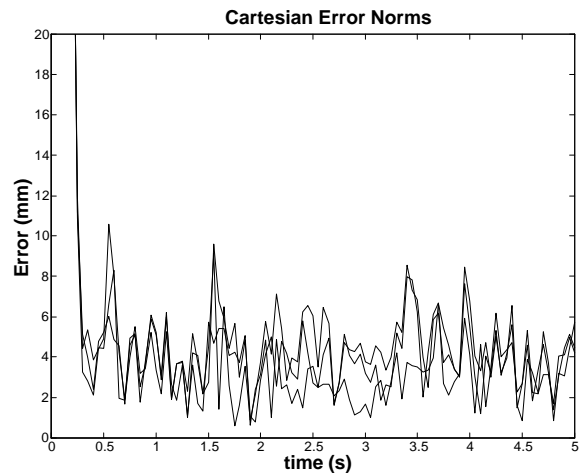


Figure 4: Cartesian error norms are show for the three target/end effector pairs as the 6-DOF robot tracks a sinusoidal target motion. The steady-state rms error is $[3.9 \ 4.5 \ 4.1]$ mm.

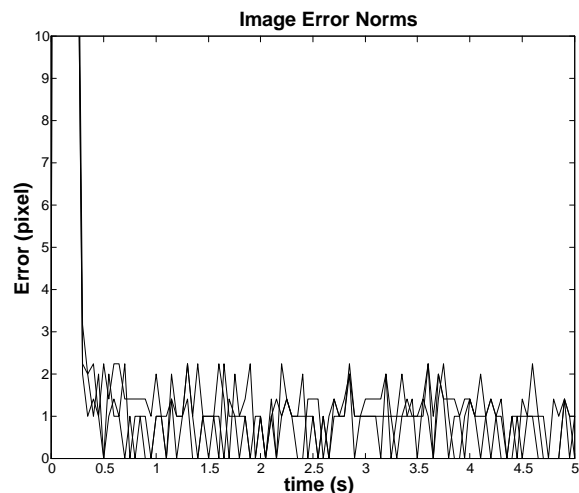


Figure 5: Image error norms are show for the three target/end effector pairs as the 6-DOF robot tracks a sinusoidal target motion. The steady-state rms error is $[1.1 \ 1.2 \ 1.1]$ pixels.

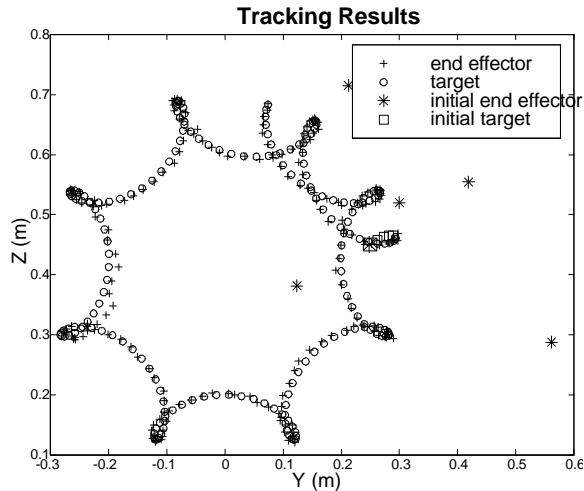


Figure 6: One target/end effector pair are shown for a 6-DOF tracking simulation. The initial target point is at (0.25,0.45). The initial 5 steps taken by the end-effector are denoted with by the ‘*’ marker. The maximum target velocity is 440 mm/s. the steady-state rms Cartesian error is 7mm; the rms image error is 1.9 pixels.

initial conditions, and improving target velocity estimates.

This paper presents a dynamic quasi-Newton control law that addresses the moving target problem for an uncalibrated image-based visual servoing system. This approach represents a significant improvement over previous efforts to track moving targets using a model independent paradigm. The result is a novel application of quasi-Newton optimization methods as applied to a time-varying objective function.

Acknowledgments

This research was supported by the State of Georgia through the Agricultural Technology Research Program in the Georgia Tech Research Institute.

References

[1] P. Allen, A. Timcenko, B. Yoshimi, and P. Michelman. Automated tracking and grasping of a moving object with a robotic hand-eye system. *IEEE Transactions on Robotics and Automation*, 2(2):152–165, April 1993.

[2] F. Chaumette and A. Santos. Tracking a moving object by visual servoing. In *IFAC 12th Tri-*

ennial World Congress, pages 643–648, Sydney, Australia, July 1993.

- [3] P. Corke and M. Good. Dynamic effects in visual closed-loop systems. *IEEE Transactions on Robotics and Automation*, 12(5):671–683, October 1996.
- [4] P. I. Corke. A robotics toolbox for matlab. *IEEE Robotics and Automation*, pages 24–32, March 1996.
- [5] J. Dennis and R. Schnabel. *Numerical Methods for Unconstrained Optimization and Nonlinear Equations*. Prentice-Hall, Englewood Cliffs, New Jersey, 1983.
- [6] R. Fletcher. *Practical Methods of Optimization*. John Wiley and Sons, 1987.
- [7] K. Hashimoto, T. Ebine, and H. Kimura. Visual servoing with hand-eye manipulator optimal control approach. *IEEE Transactions on Robotics and Automation*, 12(5):766–774, October 1996.
- [8] K. Hosoda and M. Asada. Versatile visual servoing without knowledge of true jacobian. In *IEEE/RSJ/GI International Conference on Intelligent Robots and Systems*, pages 186–193, 1994.
- [9] S. Hutchison, G.D.Hager, and P. Corke. A tutorial on visual servo control. *IEEE Transactions on Robotics and Automation*, 12(5):651–670, October 1996.
- [10] M. Jagersand. Visual servoing using trust region methods and estimation of the full coupled visual-motor jacobian. In *IASTED Applications of Robotics and Control*, 1996.
- [11] M. Jagersand, O. Fuentes, and R. Nelson. Experimental evaluation of uncalibrated visual servoing for precision manipulation. In *Proceedings of International Conference on Robotics and Automation*, 1997.
- [12] J. Piepmeier, G. McMurray, and H. Lipkin. Tracking a moving target with model independent visual servoing: A predictive estimation approach. In *IEEE International Conference on Robotics and Automation*, Leuven, Belgium, May 1998.
- [13] A. Sanderson and L. Weiss. Adaptive visual servo control of robots. In A. Pugh, editor, *Robot Vision*, chapter Adaptive Visual Servo Control of Robots, pages 107–116. Springer-Verlag, 1983.